World Academy of Science, Engineering and Technology
International Journal of Electrical and Computer Engineering
Vol:5, No:1, 2011

Simulation of a Double-Sided Axial Flux Brushless Dc Two-Phase Motor Dynamics

Abdolamir Nekoubin

Open Science Index, Electrical and Computer Engineering Vol:5, No:1, 2011 publications.waset.org/3016.pdf

Abstract**—**The objective of this paper is to analyze the performance of a double-sided axial flux permanent magnet brushless DC (AFPM BLDC) motor with two-phase winding. To study the motor operation, a mathematical dynamic model has been proposed for motor, which became the basis for simulations that were performed using MATLAB/SIMULINK software package. The results of simulations were presented in form of the waveforms of selected quantities and the electromechanical characteristics performed by the motor. The calculation results show that the two-phase motor version develops smooth torque and reaches high efficiency. The two-phase motor can be applied where more smooth torque is required. Finally a study on the influence of switching angle on motor performance shows that when advance switching technique is used, the motor operates with the highest efficiency.

Keywords**—**brushless DC motor, inverter, switching angle.

I. Introduction

CONVENTIONAL DC motors are highly efficient, however, their only drawback is that they need a commutator and brushes which are subject to wear and require maintenance. The above mentioned deficiency of the conventional solution can be overcome by the new type of DC drive based on brushless DC motors operating without mechanical transmission [1].

The brushless DC motors are permanent magnet motors where the functions of commutator and brushes were implemented by solid state switches [2]. The brushless DC motors are distinguished not only by the high efficiency but also by their no maintenance [3]. The permanent magnet motors used in this case are single phase or poly phase motors. When operating with single phase or poly phase motors, the inverter plays the role of the commutator [4]-[5]. In this paper two-phase inverters considered. The stator coils of the motor can be connected in single-phase or poly-phase systems. These connections imply the single-phase or poly-phase inverters which supply the winding. The type of winding influences the performance of the motor. The particular motor that is

Abdolamir Nekoubin is member of young researchers club Islamic Azad University, Najaf Abad Branch.
(e-mail: nekoubin@yahoo.com).

Analyzed was described in [6]. So far only single-phase and three-phase motors were considered and no study for two-phase has been done [7]. The main idea in the early stage of the PMSMs was to increase the efficiency of the traditional electric motors by permanent magnet excitation. However, the efficiency increase was not enough for the customers and the Attempts to enter the market failed [8]-[9]. Despite of this setback, several manufacturers introduced permanent-magnet machines successfully during the latest decade. Regardless of the success of radial-flux permanent-magnet machines, axial-flux permanent magnet machines, where the magnetic flux is directed axially in the air-gap and in the stator winding zone and it turns its direction in the stator and rotor core, have also been under research interest particularly due to special-application limited geometrical considerations [10]-[11]. A possibility to obtain a very neat axial length for the machine makes axial-flux machines very attractive into applications in which the axial length of the machine is a limiting design parameter. Such applications are, for example electrical vehicles wheel motors and elevator motors. Axial flux machines have usually been used in integrated high-torque applications [12]-[13]. AFPM motors can be designed as double sided or single sided machines, with or without armature slots, with internal or external rotors and with surface mounted or interior type permanent magnets (PMs). Low power AFPM machines are usually machines with slot less windings and the surface mounted PMs [14]-[15]-[16]. In this paper the calculations were done for the particular motor which was designed as a water pump with the wet rotor.

II. Axial Flux Permanent Magnet Motor Structure

Several axial-flux machine configurations can be found regarding the stator(s) position with respect to the rotor(s) positions and the winding arrangements giving freedoms to select the most suitable machine structure into the considered application. The object of study in this paper is double-sided AFPM brushless machine with internal salient-pole stator and two external rotors shown in Figure. 1.

It is more compact than the motor with internal rotor. The double-sided rotor with PMs is located at the two sides of the stator. The stator consists of the electromagnetic elements made of ferromagnetic cores and coils wound on them. These elements are placed axially and uniformly distributed on the stator circumference and glued together by means of synthetic resin. The stator coils can be connected in single-phase and

multi-phase systems. The motor of particular winding connection exhibits its unique performance that differs it from the motors of the other connection systems.

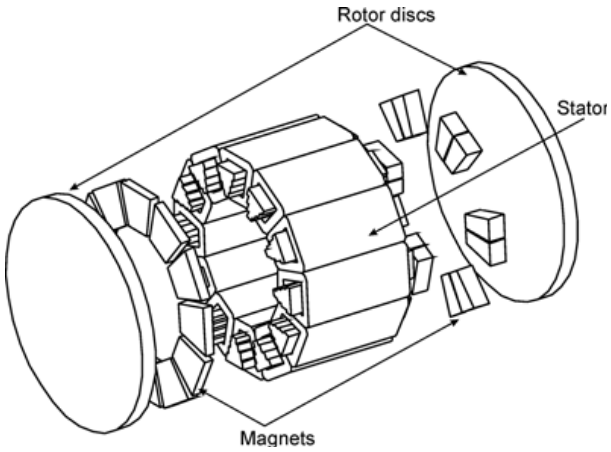

Fig 1 Double-sided AFPM motor with two external rotors

In this paper motor with two-phase is studied and are analyzed. On both sides of the stator are the rotors made of steel discs with the permanent magnets glued to the disc surfaces. The distribution of the magnets on the rotor discs has to be adequate to the stator poles polarity. The stator winding in this case is connected as shown in Figure.2. Here the coils of phases A and B are alternatively connected.

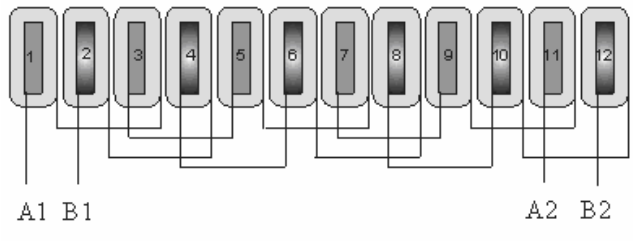

Fig. 2 Windings of the stator is connected in Two - phase

III. Mathematical Model of the Supply–Inverter–Motor System

The supply-inverter-motor circuit model is shown in Figure.3.

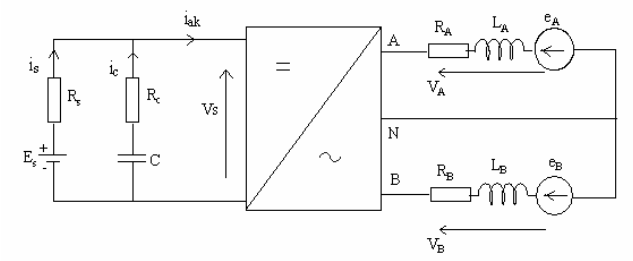

Fig. 3 Circuit diagram of supply-inverter-motor system

The circuit parameters are set up under the following assumptions:

· All elements of the motor are linear and no core losses are considered,

· Electromotive force ea and cogging torque vary sinusoidally with the rotational electric angle θe

· Due to the surface mounted permanent magnets winding inductance is constant (does not change with the θe angle),

· Voltage drops across diodes and transistors and connecting wire inductance are ignored.

The equations that describe the model are as follows:

Voltage equation at the source side

$$E_b - i_s.R_b - i_c.R_c = 0 \quad (1)$$

$$V_s = V_c + i_c.R_c \quad (2)$$

$$i_s = i_{sk} + i_c \quad (3)$$

Where: Eb and Rb :voltage and resistance of the source, Rc: capacitor resistance, i_s: source circuit current, i_{sk}: converter input current, v_c: voltage across capacitor.:

$$V_c = \frac{Q_c}{C} \quad (4)$$

Qc: charge in capacitor, C: capacitance, i_c: current flowing through the capacitor:

$$i_c = \frac{dQ_c}{dt} \quad (5)$$

Voltage equations at the motor side (Figure 4) are:

$$V_A = V_{SA} \quad (6)$$

$$V_B = V_{SB} \quad (7)$$

where:

v_{sA}, v_{sB}, are the inverter output voltages that supply the 2 – phase winding, v_A, v_B, are the voltages across the motor armature winding.

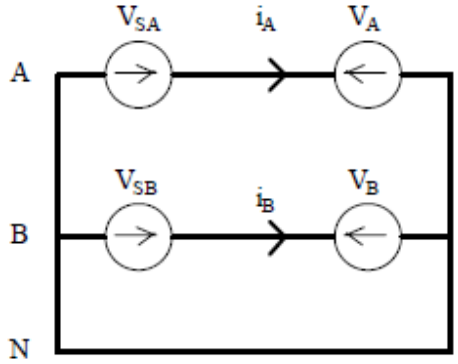

Fig. 4 Scheme to the equations6,7

The equation of the voltages across the motor winding

$$\begin{bmatrix} V_A \\ V_B \end{bmatrix} = \begin{bmatrix} R_A & 0 \\ 0 & R_b \end{bmatrix} \begin{bmatrix} i_A \\ i_B \end{bmatrix} + \frac{d}{dt} \begin{bmatrix} L_A & L_{AB} \\ L_{BA} & L_B \end{bmatrix} \begin{bmatrix} i_A \\ i_B \end{bmatrix} + \begin{bmatrix} e_A \\ e_B \end{bmatrix} \quad (8)$$

or in shortened version:

$$V_a = R_a.I_a + \frac{d}{dt} l_a.I_a + E_a \quad (9)$$

Open Science Index, Electrical and Computer Engineering Vol:5, No:1, 2011 publications.waset.org/3016.pdf

Open Science Index, Electrical and Computer Engineering Vol:5, No:1, 2011 publications.waset.org/3016.pdf

Since the resistances Ra of all phases are the same:

$$R_a = \begin{bmatrix} R_a & 0 \\ 0 & R_a \end{bmatrix} \tag{10}$$

Here there is no mutual inductance between the phases A and B, they are displaced by 90^0 . So, L_{AB} , $L_{BA} = 0$.
Due to the symmetrical winding the inductances $L_A = L_B = L$
The inductance matrix takes the form:

$$L_a = \begin{bmatrix} L & 0 \\ 0 & L \end{bmatrix} \tag{11}$$

$$i_a + i_b = 0 \tag{12}$$

Thus the voltage equation takes the form:

$$\begin{bmatrix} V_A \\ V_B \end{bmatrix} = \begin{bmatrix} R_A & 0 \\ 0 & R_B \end{bmatrix} \begin{bmatrix} i_A \\ i_B \end{bmatrix} + \frac{d}{dt} \begin{bmatrix} L & 0 \\ 0 & L \end{bmatrix} \begin{bmatrix} i_A \\ i_B \end{bmatrix} \begin{bmatrix} e_A \\ e_B \end{bmatrix} \tag{13}$$

The electromotive force induced in the phase A winding:

$$e_a = K_E \omega_m \sin(\theta_e) \tag{14}$$

The electromotive force induced in the phase B winding is given by:

$$e_b = K_E \omega_m \sin(\theta_e - 90^\circ) \tag{15}$$

Where: K_E: constant, ω_m: rotor angular speed:

$$\omega_m = \frac{1}{P} \frac{d\theta_e}{dt} \tag{16}$$

θe: electrical angle, p: number of pole pairs for two-phase winding, the electromotive forces written in a form of matrix Ea:

$$E_a = \frac{K_E}{P} \begin{bmatrix} \sin\theta_e \\ \\ \sin(\theta_e - \frac{\pi}{2}) \end{bmatrix} \frac{d\theta_e}{dt} \tag{17}$$

Equation that links the supply and motor sides:

$$i_{SK} = \frac{1}{V_S}(i_A V_{SA} + i_B V_{SB}) \tag{18}$$

results from the equality of the powers at input and output of the inverter. Supply voltages for the phases (v_{sA}, v_{sB}) results from the operation of converter. The mechanical system with all torques is shown schematically in Figure. 5. This system is defined by the following equation 19.

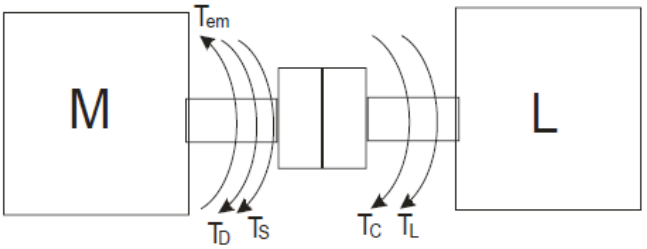

Fig. 5 Mechanical system with torques

$$T_{em} = TJ + TD + Ts + Tc + TL \tag{19}$$

The torque components of equation 19 are expressed by the following equations.
Inertia torque:

$$TJ = J \frac{d\omega m}{dt} \tag{20}$$

Viscous friction torque:

$$TD = D.\omega_r \tag{21}$$

Coulomb friction torque:

$$Ts = sign(\omega r)Td \tag{22}$$

Cogging torque:

$$Tc = Tmc \sin(\varphi_e + \beta) \tag{23}$$

Load torque: T_L
The electromagnetic torque is given by following equation 24 and 25:

$$T_{em} = \frac{e_{AiA}}{\omega_\gamma} + \frac{e_{BiB}}{\omega_\gamma} \tag{24}$$

$$T_{em} = \frac{e_{AiA}}{\omega_R} + \frac{e_{BiB}}{\omega_R} = K_e(f_a(\theta_e).i_A + f_b(\theta_e).i_B \tag{25}$$

Where:

$$f_a(\theta_e) = \sin(\theta_e\ ) \tag{26}$$

$$f_b(\theta_e) = \sin(\theta_e - \frac{\pi}{2}) \tag{27}$$

Combining all the above equations, the system in steady-space form is:

$$x\cdot = Ax + Bu \tag{28}$$

$$x = \begin{bmatrix} i_A & i_B & \omega_\gamma & \theta_e \end{bmatrix}^t \tag{29}$$

$$A=\begin{bmatrix} \frac{-R_S}{L} & 0 & -\frac{K_E\ (f_a(\theta_e))}{L} & 0 \\ 0 & \frac{-R}{L} & -\frac{K_E(f_a(\theta_e))}{L} & 0 \\ \frac{K_E(f_a(\theta_e))}{J} & \frac{K_E(f_b(\theta_e))}{J} & -\frac{D}{J} & 0 \\ 0 & 0 & \frac{P}{2} & 0 \end{bmatrix} \quad (30)$$

$$B=\begin{bmatrix} \frac{1}{L} & 0 & 0 \\ 0 & \frac{1}{L} & 0 \\ 0 & 0 & \frac{-1}{J} \\ 0 & 0 & 0 \end{bmatrix} \quad (31)$$

$$u=\begin{bmatrix} V_A & V_B & T_L \end{bmatrix}^t \quad (32)$$

Equation of the motor efficiency is:

$$Eff\% = \frac{P_{out}}{P_{in}}.100\% \quad (33)$$

The average input power:

$$P_{in} = \frac{1}{T}\int_0^T (V_s.i_{ak})dt \quad (34)$$

The average output power:

$$P_{out} = \frac{1}{T}\int_0^T (T_L.\omega)dt \quad (35)$$

IV. Dynamic Simulation of the Motor

The simulation of the motor operation in dynamic conditions was done using software package MATLAB/SIMULINK®. To simulate this operation, it was assumed that: the drive system is supplied with constant voltage of 300 *V*, the system is loaded with the rated torque of 6.1 N.m,. The simulation results of starting of the motor are shown in Figs 6, 7, 8, 9 and 10. In particular the Figure.6 shows the rotary speed waveform. The ripple in the speed waveform is due to the oscillation of motor torque. It consists of two components: electromagnetic torque Tem and cogging torque Tc. These two components are shown in Figure 10, which were drawn when the motor reached steady state. The electromagnetic torque waveform obtained during the starting process is shown in Figure 9. The results presented in Figure.10 show that the torque developed by the motor is always positive despite the relatively big cogging components. This positive resultant torque is obtained due to displacement of PMs on one of the rotor discs.

TABLE I
PARAMETERS OF ELECTRIC CIRCUITE AND MECHANICAL SYSTEM

Symbol	Quantity	Values
E_b	emf of the battery	300 *V*
R s	source Resistance	1.5 Ω
R c	resistance in series with capacitor	2 Ω
C	capacitance	10μ *F*
R a	phase resistance of the brushless DC motor	8 Ω
L c	phase inductance of the brushless DC motor	0.021H
K e	emf constant	1.324
J	moment of inertia	0.001 *Kg /m*2
D	friction coefficient	0.001 N/(rad/s)
T load	load torque	2.2 *N. m*
T mc	maximum cogging torque	0.3 *N.m*
T s	coulomb friction torque	0.1 *N.m*

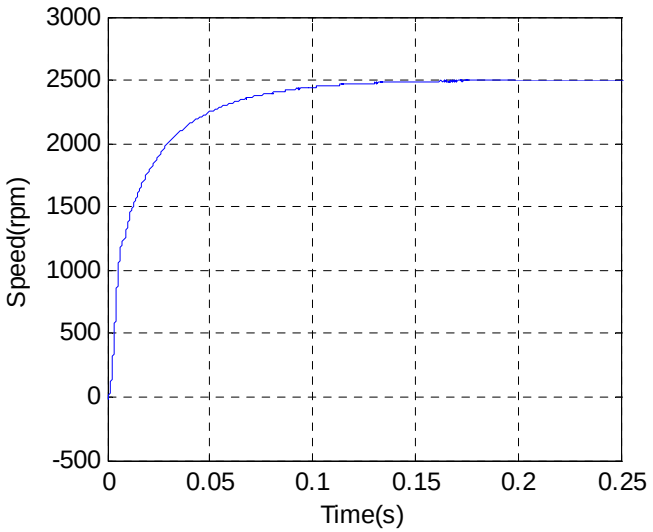

Fig. 6 Waveform of rotary speed

Open Science Index, Electrical and Computer Engineering Vol:5, No:1, 2011 publications.waset.org/3016.pdf

Open Science Index, Electrical and Computer Engineering Vol:5, No:1, 2011 publications.waset.org/3016.pdf

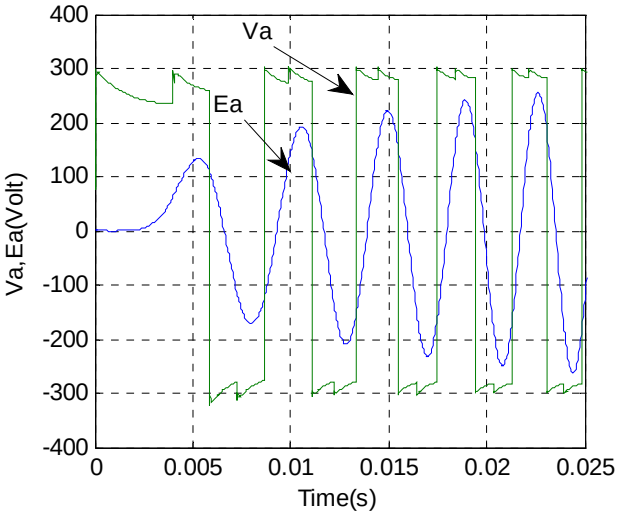

Fig. 7 Waveform of EMF (Ea) and armature voltage (Va)

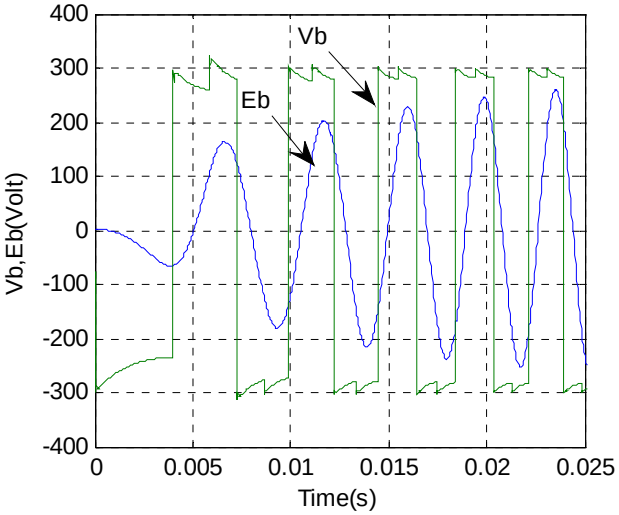

Fig. 8 Waveform of EMF (Eb) and armature voltage (Vb

The waveform of EMF (Ea) and armature voltage (Va) of phase A and the waveform of EMF (Eb) and the armature voltage (Vb) of phase B are shown in Figs 7. and 8. The induced EMF's and voltage applied to the motor are in phase because the winding was switched ON without any delay with respect to the position of magnets and winding.

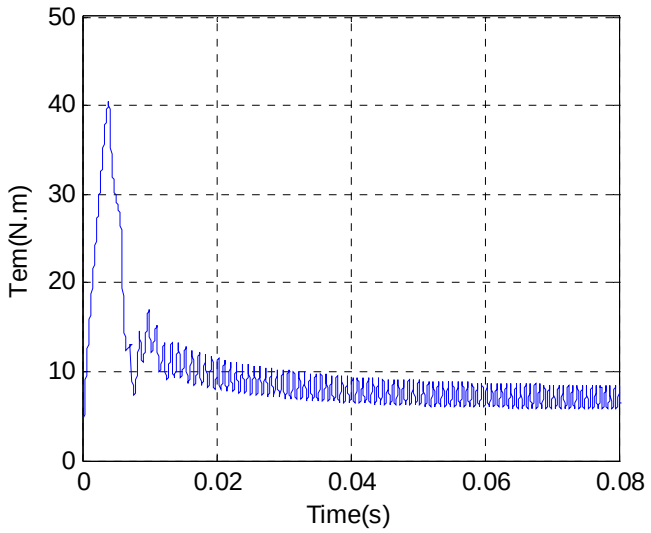

Fig. 9 Waveform of electromagnetic torque (Tem)

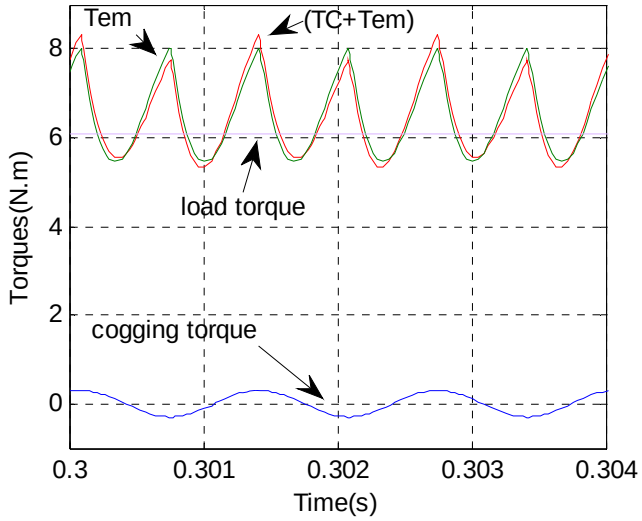

Fig. 10 Waveforms of electromagnetic torque, cogging torque and resultant torque

V. Influence of Switching Angle on Motor

Due to the high-speed operation, the winding inductance causes a significant phase delay in the current waveform. The results in the current and the emf waveforms being out of phase, and a negative torque component is generated, with a consequent reduction of the overall torque. In order to get motor better performance Phase commutation advanced is often employed. In DC brush motor the commutation angle is determined by the position of brushes and is kept constant. In BLDC motors the switching angle may vary accordingly to the controller of the inverter that is used.

The inverter considered for the brushless motor with two-phase winding is shown in (Fig.11). The position sensors are placed between the coils in the intervals of 90 degree .These

sensors sense the position of the rotor and they trigger the transistors so that they switch on the respective stator winding.

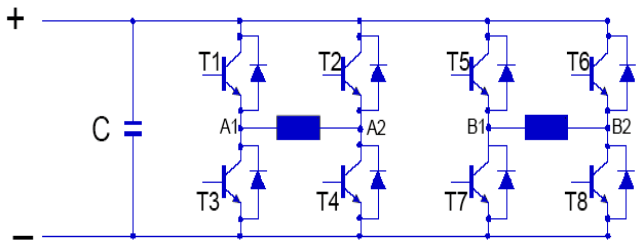

Fig. 11. Inverter considered for BLDC with Two-Phase Winding

As the switching angle is advanced, the difference between back-emf and the supply voltage increases, and the torque thereby increases. However, there exists an optimal advanced angle, beyond which the drive performance deteriorates. The simulation was done for the following switching angles $\beta = -20^\circ, -30^\circ, -40^\circ, -45^\circ$

The results of simulation were plotted in the form of characteristics of average values of the efficiency, input current and mechanical power output shown in Figs 12, 13 and 14. The characteristics were drawn in the MATLAB from the results obtained in simulation using dynamic model of the motor. The efficiency was calculated as same as section. III. The motor efficiency is maximum when the switching angle $\beta = -40^\circ$, which means transistors are switched much earlier and the motor efficiency is minimum when $\beta = -20^\circ$.

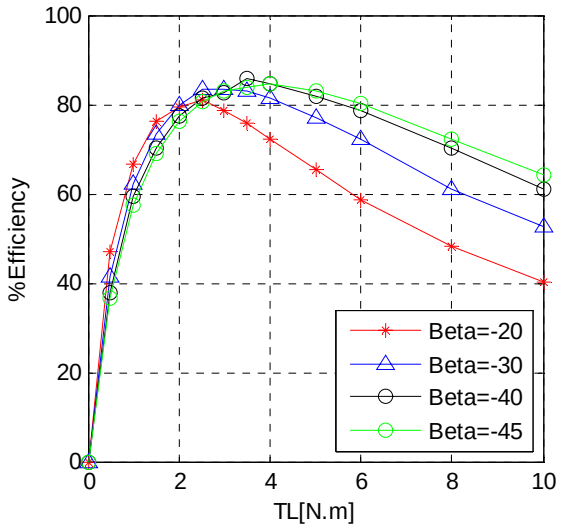

Fig. 12 Efficiency (Eff) vs. load torque(TL)

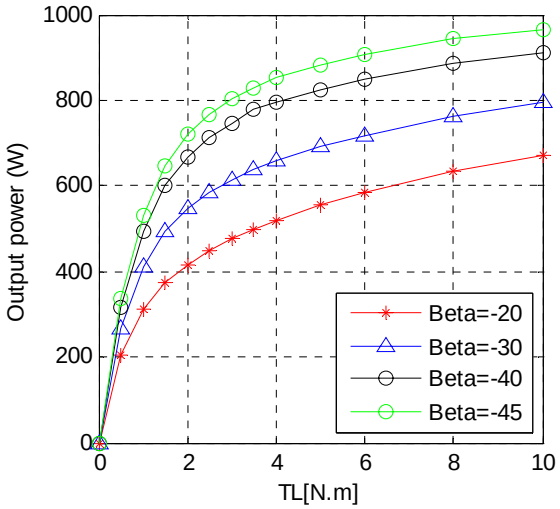

Fig. 13. Mechanical power output (Pem) vs. load torque (TL)

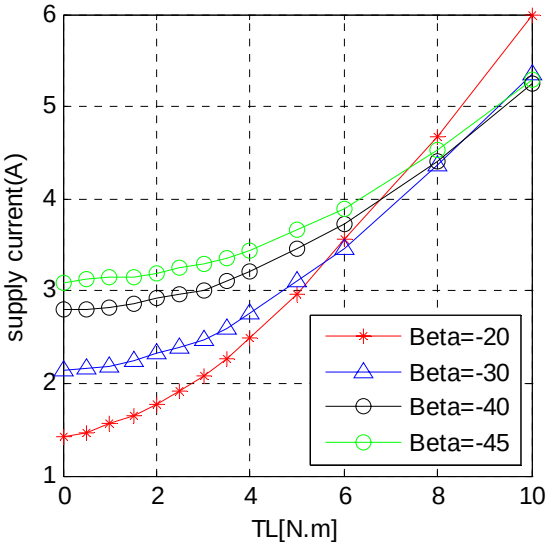

Fig. 14 Input current (Is) vs. load torque(TL)

VI. Conclusion

The performance of the AFPM BLDC motor with two-phase winding was analyzed in this paper. To study the motor operation, a mathematical dynamic model has been proposed. This model became the basis for block diagram and simulations, which was performed using MATLAB/SIMULINK software package. The results obtained from dynamic model enabled to deduct the following conclusions:

- The two-phase motor develops the torque with low ripple
- The results of simulation at rated torque show the AFPM motor with two-phase winding has high efficiency
- In two-phase motor two sensors and 8 transistors are necessary which makes the circuit complex.

A study done on the influence of switching angle on motor

Open Science Index, Electrical and Computer Engineering Vol:5, No:1, 2011 publications.waset.org/3016.pdf

performance shows that motors operate better when the windings are switched ON earlier with respect to the emfs induced in them. It means the inverters should operate at the advanced switching angle if voltage inverters are applied.

REFERENCES

[1] shak, D. Manap, N.A.A. Ahmad, M.S. Arshad, M.R., Electrically actuated thrusters for autonomous underwater vehicle, *Advanced Motion Control, 11th IEEE International Workshop, Vol. 32, pp. 619- 624, 21-24March2010.*

[2] Jong Hyun Choi, Jung Hoon Kim, Dong Ho Kim, Design and Parametric Analysis of Axial Flux PM Motors with Minimized Cogging Torque, *IEEE Transactions on Magnetics, Vol. 45, pp. 2855 - 2858 19 May. 2009.*

[3] Guoping Peng, Research on energy conversion control for small-scaled brushless DC wind power system, *IEEE Transaction Control System, vol. 9 n. 4, July 2004, pp. 629–636.*

[4] Fengge Zhang, Nikolaus Neuberger, Eugen Nolle, Peter Gruenberger, Fengxiang Wang, A New Type of Induction Machine with Inner and Outer Double Rotors, *IEEE International Conference on Power Electronics and Motion Control, Vol. 1, pp. 286-289, Jan. 2004.*

[5] K. T. Chau, Y. B. Li, J. Z. Jiang and S. X. Niu, Design and control of a PM brushless hybrid generator for wind power application, *IEEE Transaction on Magnetics, Vol. 42, n. 10, pp.349−356 ,6-8 September 2006.*

[6] D. Zhang, K.T. Chau, S. Niu and J.Z. Jiang, Design and analysis of a double-stator cup-rotor PM integrated-starter-generator*, IEEE IASAnnual Meeting, pp. 20-26, Feb. 2006.*

[7] Y. Zhang, K. T. Chau, J. Z. Jiang and D. Zhang, A finite element analytical method for electromagnetic field analysis of electric machines with free rotation, *IEEE Transaction on Magnetics, Vol. 42 n. 10, January 2006, pp. 303−309.*

[8] Ghazanfar Shahgholian, Jawad Faiz, Navid Sedri, Pegah Shafaghi, *Mehdi Mahdavian*, *Design and Experimental Analysis of a High Speed Two-Phase Induction Motor Drive for Weaver Machines Applications*, International Review of Electrical Engineering (IREE), Vol. 5 N. 2, April 2010, pp. 106-112.

[9] Jang, S.-M., H.-W. Cho, and S.-K. Choi," Design and analysis of at high speed brushless DC motor for centrifugal compressor," *IEEE Transactions on Magnetics, Vol. 43, No. 6, 2573-2575*, *June* 2007.

[10] Rabinovici, R., Magnetic field analysis of permanent magnet motors," *IEEE Transactions on Magnetic*, *Vol. 32, No. 1, 265-269, January 1996.*

[11] Qiu, Z.-J., J.-D. Xu, G. Wei, and X.-Y. Hou, "An improved time domain finite element-boundary integral scheme forelectromagnetic scattering from 3-D objects," *Progress InElectromagnetics Research*, *PIER 75, 119-135, 2007.*

[12] C. Depollier,"The three exact components of the magnetic field createdby a radially magnetized tile permanent magnet," *Progress In Electromagnetics Research, PIER 88, 307*-319, 2008.

[13] K. Atallah and D. Howe, "A novel high performance magnetic gear,*" IEEE Trans. on Magnetics, Vol. 37, No. 4, pp. 2844−2846, 2001.*

[14] R. Datta and V.T. Ranganathan, "A method of tracking the peak power points for a variable speed wind energy conversion system," *IEEE Trans. on Energy Conversion, Vol. 18, No. 1, pp. 163−168, 2003.*

[15] Z. Q. Zhu and D. Howe," Influence of design parameters on cogging torque in permanent magnet machines, "*IEEE Trans. on Energy Conversion, Vol. 15, No. 4, pp. 407−412, 2000.*

[16] Wang Fengxiang; Wang Jiqiang, Kong Zhiguo, Zhang Fengge," Radial and Axial Force Calculation of BLDC Motor with Passive Magnetic Bearing, *Proceedings of ICIEA* 2007 pp.618-621. 23-25 May 2007.

[17] Fengge Zhang, Guangwei Liu, Yongshan Shen, "Characteristic Study on a Novel PMSM with Opposite-rotation Dual Rotors," *Proceeding of International Conference on Electrical Machines and Systems, vol. 50, no. 5, pp. 920–935 8-11 Oct. 2007.*

[18] M. Jafarboland, A. A. Nekoubin, Design and Optimization of a Double-Sided Linear Induction Based on Finite Element Method, International Review of Electrical Engineering (IREE), Vol. 5 n. 3, June 2010, pp. 116-124.

Abdolamir Nekoubin was born in Iran, in1985. He received the B.S. degree in 2007 and the M.S. degree in 2009, all in electrical engineering from Islamic Azad University, Najaf Abad Branch. His current research interests include induction motor, linear induction motor, and nonlinear control theory. Currently he is member of young researchers club.

Open Science Index, Electrical and Computer Engineering Vol:5, No:1, 2011 publications.waset.org/3016.pdf